

Supporting Information

Mass spectrometric detection of fleeting neutral intermediates generated in electrochemical reactions

Jilin Liu^[a, b, c], Kai Yu^[a, b], Hong Zhang^[a, b], Jing He^[a, b, c], Jie Jiang^{*[a, b, c]} and Hai Luo^{*[d]}

[a]School of Environment, School of Marine Science and Technology (Weihai), Harbin Institute of Technology, Weihai, Shandong, 150090, China,

[b] State Key Laboratory of Urban Water Resource and Environment, Harbin Institute of Technology, Harbin, Shandong 150090, China

[c]School of Chemistry and Chemical Engineering, Harbin Institute of Technology, Harbin 150001, China

[d]Beijing National Laboratory for Molecular Sciences, College of Chemistry and Molecular Engineering, Peking University, Beijing, 100871, China.

E-mail: jiejia@hitwh. edu. cn, hluo@pku. edu. cn

Table of Contents

Experimental Section3

Identification of the electrochemical formation of TPrA^{•+}6

Identification of the electrochemical formation of Ru(bpy)₃⁺10

Identification of the electrochemical formation of TPrA[•]11

Identification of the electrochemical formation of DBAE^{•+}16

Identification of the electrochemical formation of DBAE[•]19

Identification of the electrochemical formation of TEA^{•+}22

Identification of the electrochemical formation of TEA[•]25

Experimental Section

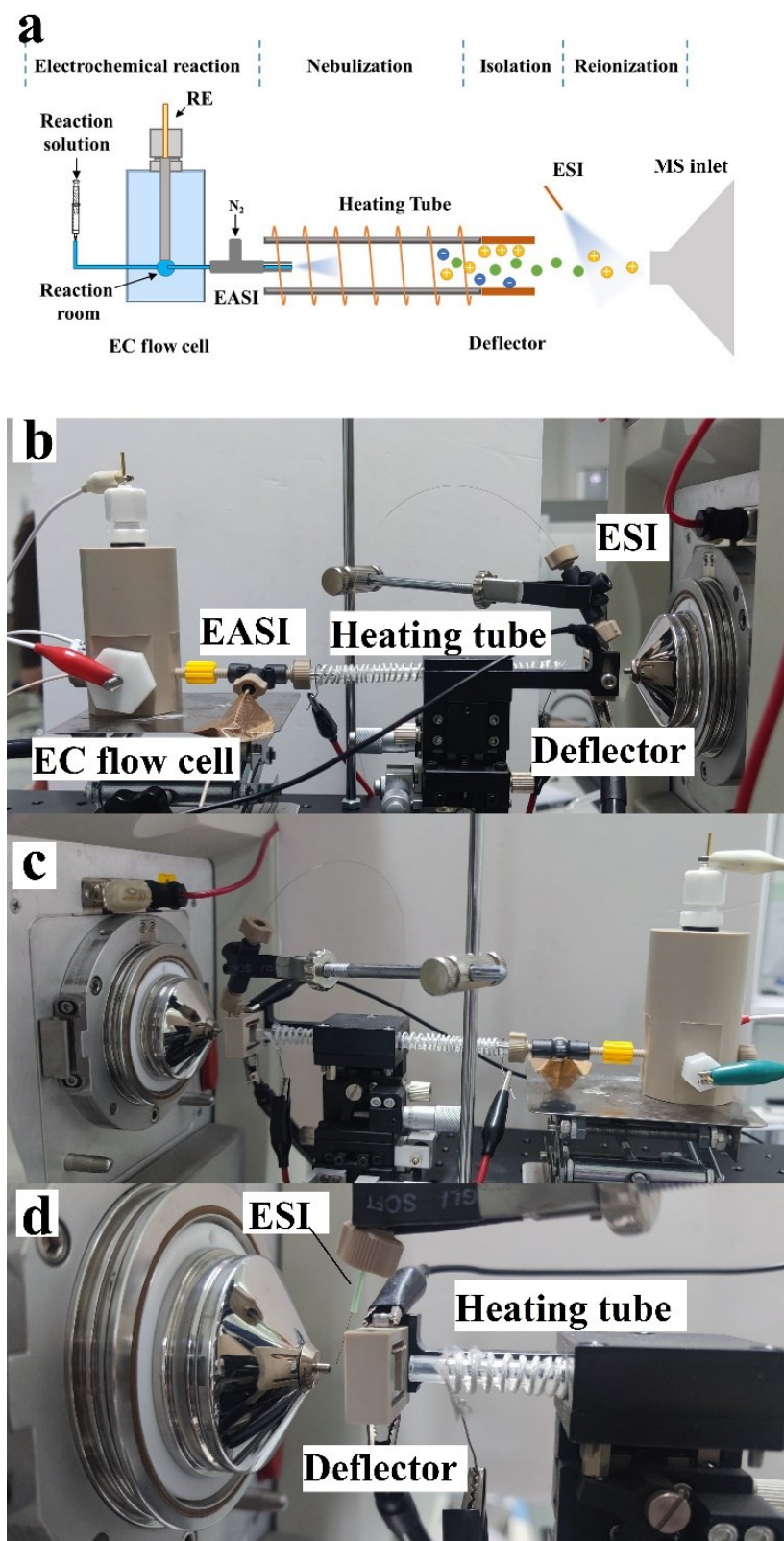


Fig. S1 The a) Schematic diagram, b) right view, c) left view photograph of EC-NR-MS setup and d) detailed photograph of NR setup.

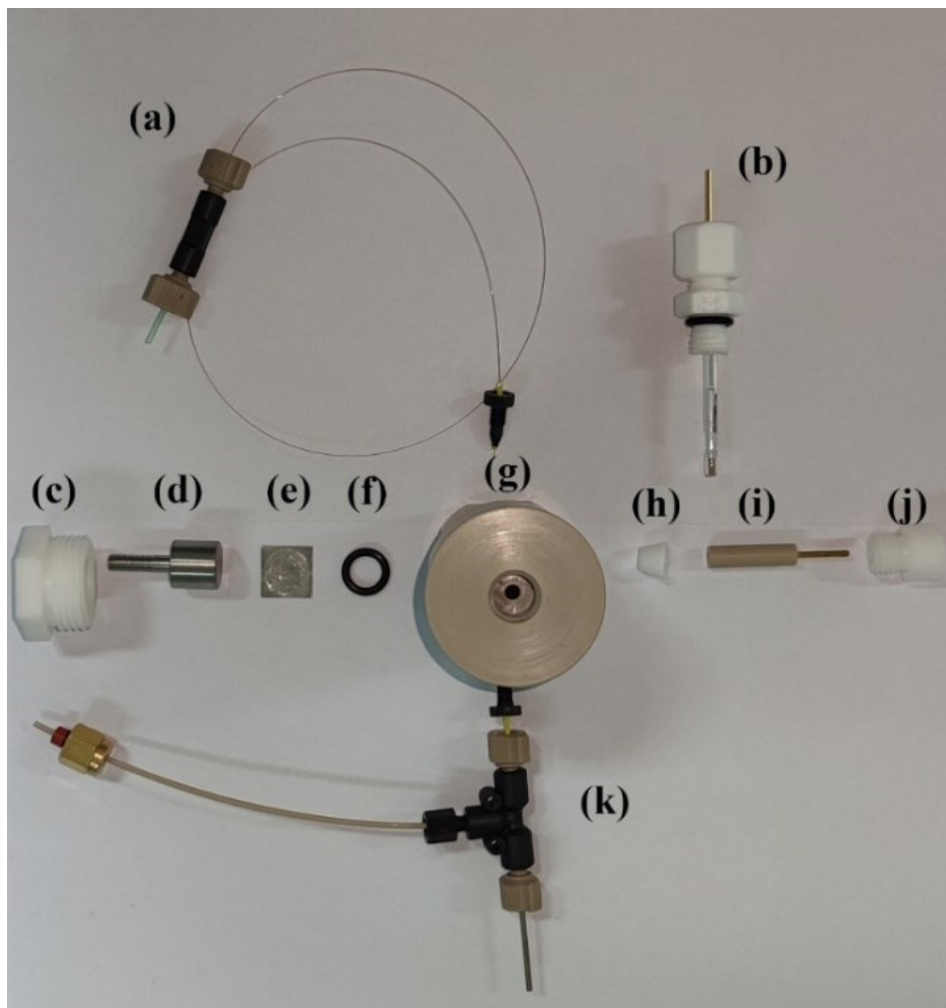


Fig. S2 Photograph of the EC flow cell and EASI source after disassembly a) injection capillary, b) reference electrode, c) block rotary knob, d) block ingot, e) platinum plate counter electrode, f) rubber gasket, g) electrochemical cell, h) gasket, i) glass carbon disk working electrode, j) block rotary knob, k) sonic spray ionization sprayer.

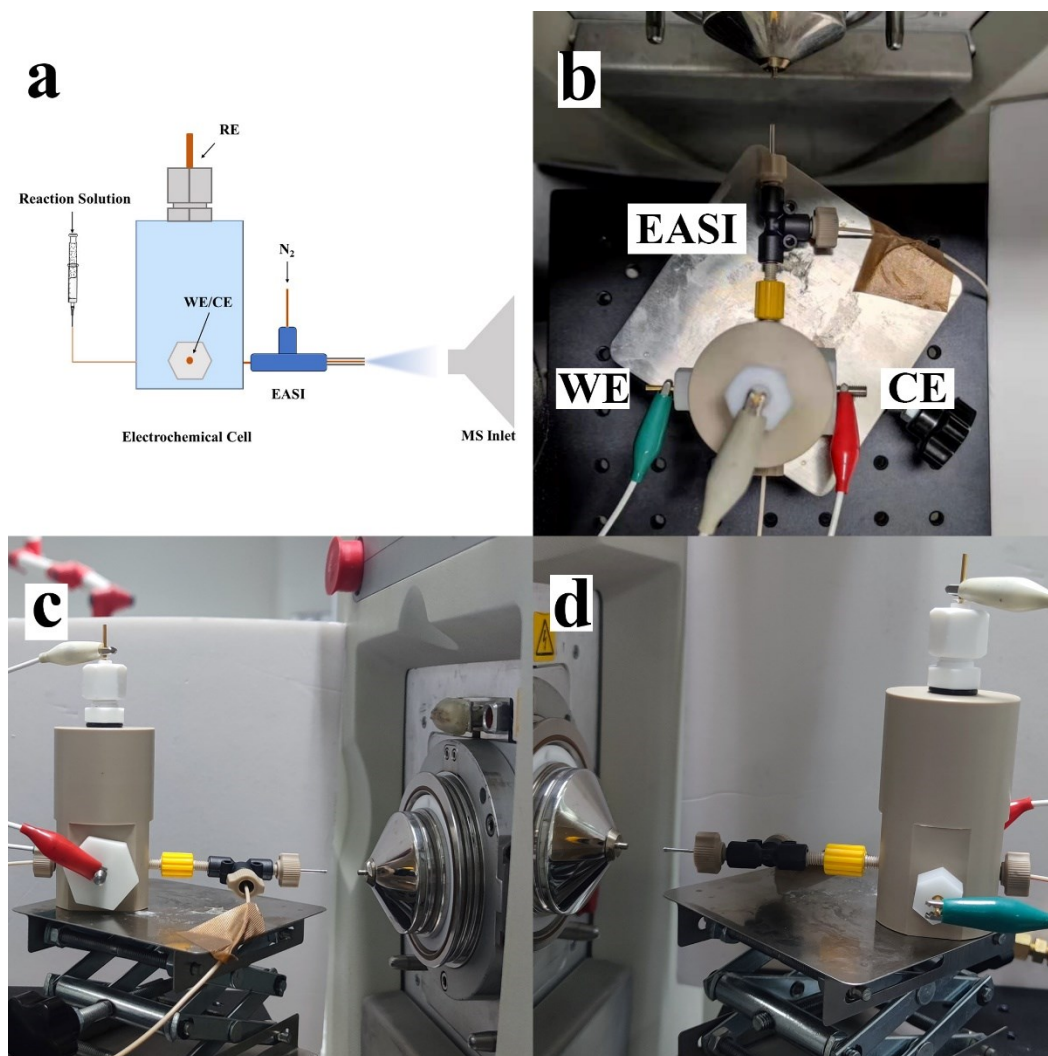
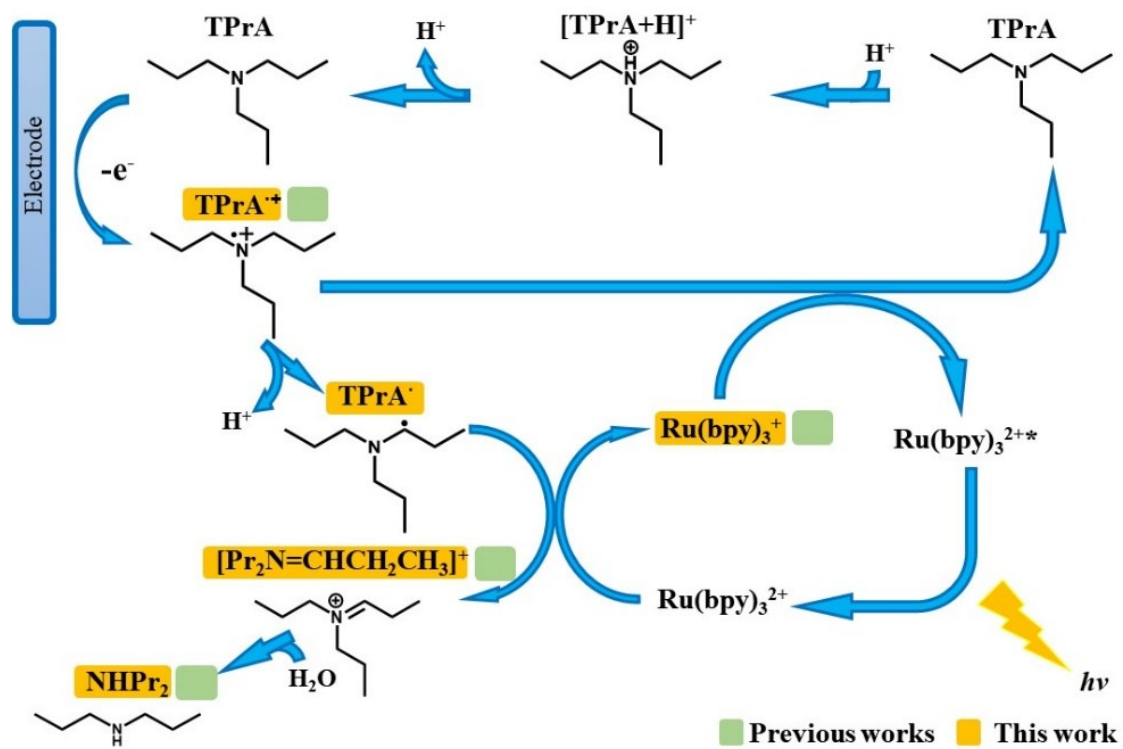


Fig. S3 The a) Schematic diagram, b) vertical view, c) right view and d) left view photograph of EC device.

Identification of the electrochemical formation of TPrA^{•+}



Scheme S1 ECL pathway of Ru(bpy)₃²⁺/TPrA system at low oxidation potential of 0.8 V.

Prior to the MS experiments, the electrochemical response of 100 ppm TPrA in 1 mM PBS aqueous solution (pH=7.5) was characterized by cyclic voltammetry (CV) in the EC flow cell (glassy carbon as working electrode, platinum as counter electrode and Ag/AgCl as reference electrode). As shown in Fig. S4a, the oxidation peak of TPrA appeared at 0.8 V, which is similar to that shown in the work of Bard et al.¹ Hence, the customized EC flow cell can precisely achieve such electrochemical reaction on demand. Considering that the half-life of radical cations, a short distance between the EC flow cell and MS inlet is essential. Therefore, only the EC flow cell/EASI unit was placed in front of mass spectrometer for capturing the radical cations. Thereafter, the MS signal of TPrA solution was determined, only two peaks appeared on the mass spectrum (Fig. S4b). The major one at m/z 144 is ascribed to the protonated TPrA while another at m/z 102 is the protonated NHPr₂. Although NHPr₂ is the oxidation product of TPrA (see Scheme S1),² its existence may be due to the impurity of the commercial reagent. By holding the working electrode potential at 0.8 V, the relative intensity of peak m/z 102 increased significantly in Fig. S4c than in Fig. S4b, indicating the generation of NHPr₂ during the reaction. Also in Fig. S4c, two new peaks came out at m/z 142 and 143, corresponding to the intermediate ion [Pr₂N=CHCH₂CH₃]⁺ and radical cation TPrA^{•+}, respectively. Fig. S5 (in Supporting information) illustrates the isotopic peak (also at m/z 143) of [Pr₂N=CHCH₂CH₃]⁺ (m/z 142) with a theoretical relative abundance of 9.73% (red line), which is much lower than that of experimentally measured radical cation peak (58.75%, blue line). Meanwhile, the structural characterization of [TPrA+H]⁺, TPrA^{•+} and [Pr₂N=CHCH₂CH₃]⁺ were achieved by tandem mass spectrometry (MS²). As can be seen in Fig. S6a (Supporting information), the fragmentation patterns of these three ions are consistent with the previous report.³ It should be pointed out that TPrA^{•+} is determined for the first time with EC-MS by precise control of the electrooxidation potential at 0.8 V.

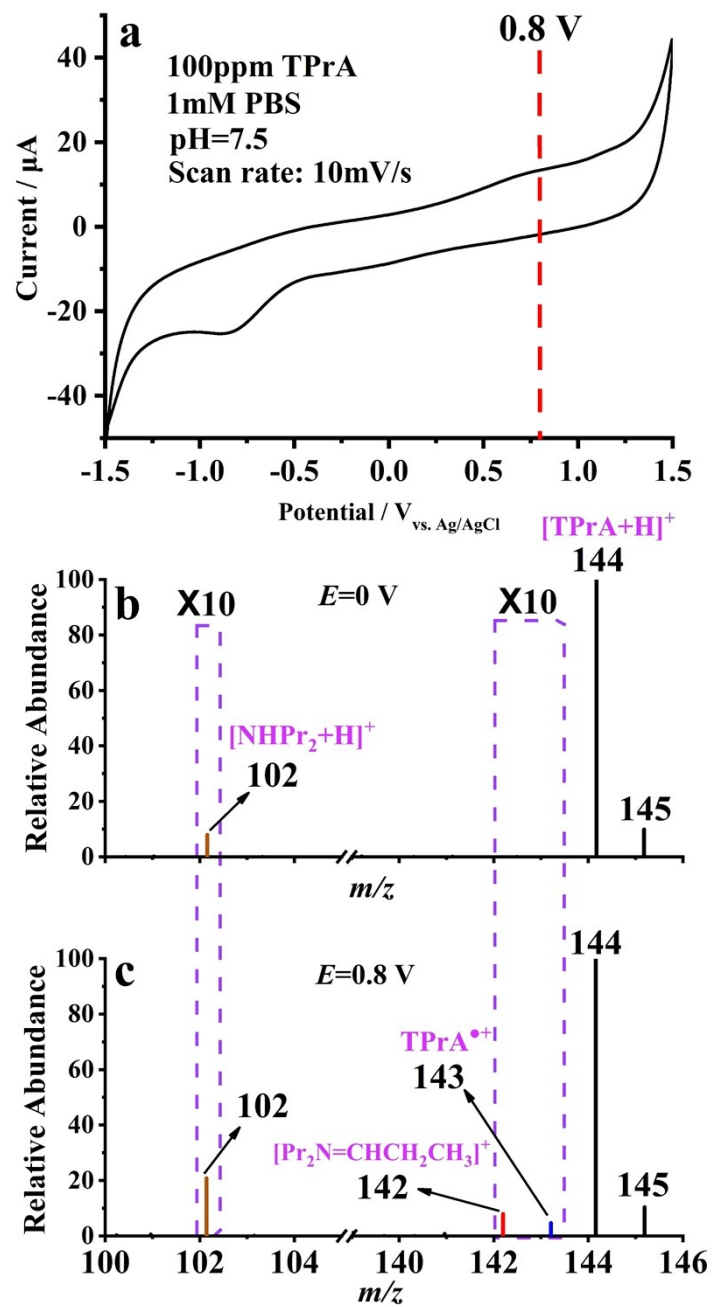


Fig. S4 (a) Cyclic voltammogram of 100 ppm TPrA in aqueous 1 mM PBS buffer, pH=7.5, scan rate=10 mV/s; MS spectra of solution (a) obtained at electrooxidation potential (E) of (b) 0 V and (c) 0.8 V.

TPrA sample solution (100 ppm, pH=7.5) was prepared with nitrogen-saturated purified water and PBS buffer (1 mM, pH=7.5). The sample solution was injected into the EC cell at a fixed flow rate of 25 $\mu\text{L}/\text{min}$. The applied oxidation potential to working electrode was 0.8 V with respect to the reference electrode (vs. Ag/AgCl reference electrode). The distance from EASI sprayer tip to the MS inlet was ca. 9 mm and the gas pressure of EASI was ca. 60 psi.

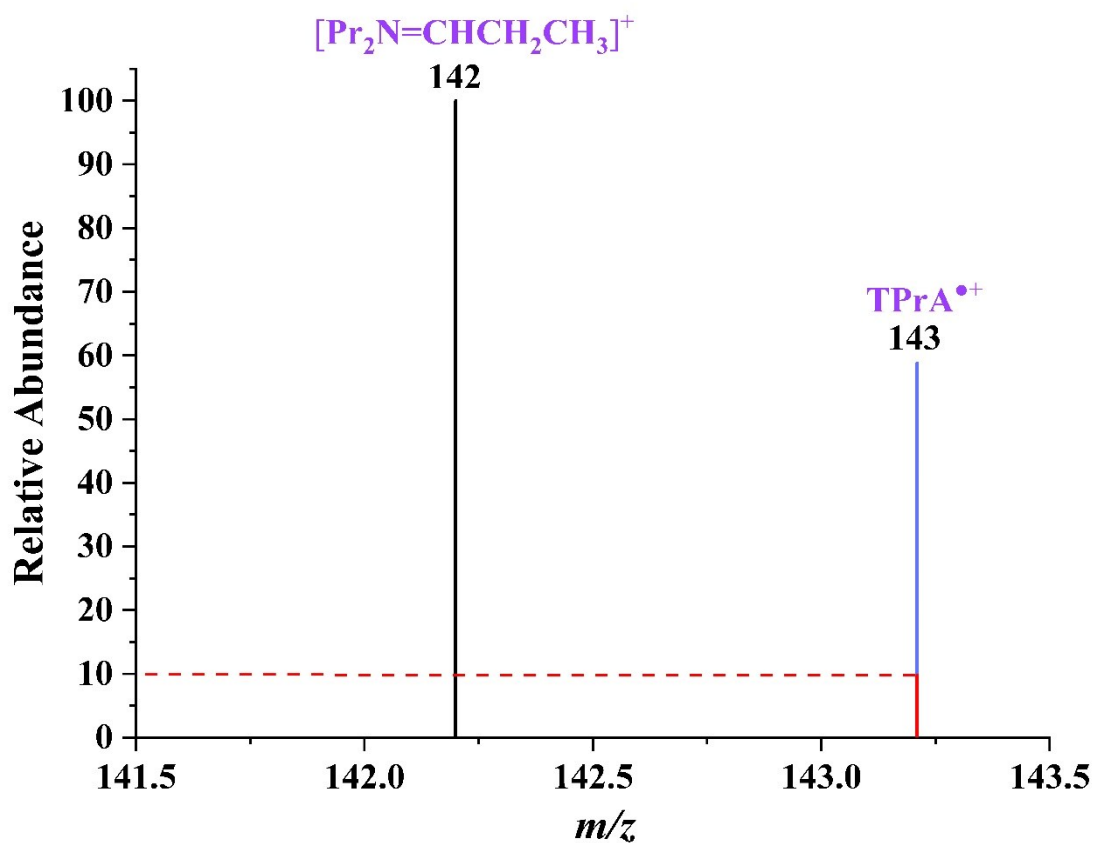


Fig. S5 Relative abundance comparison between the isotopic peak of $[\text{Pr}_2\text{N}=\text{CHCH}_2\text{CH}_3]^+$ (red line) and the experimentally obtained peak of $\text{TPrA}^{\bullet+}$ (blue line).

As can be seen in Fig. S6a., [TPrA+H]⁺ shows facile fragmentation by loss of propylene (at *m/z* 102), and a small peak at *m/z* 60 is owing to the additional propylene loss. Different from the CID of [TPrA+H]⁺, MS² of TPrA^{•+} generated typical fragments of *m/z* 114, 101, 100 and 58 (Fig. S6b, Supporting information). The ions at *m/z* 114 and 100 are due to the loss of one CH₃CH₂[•] and one C₃H₇[•] from TPrA^{•+}, respectively. Ion *m/z* 101 is assigned to the loss of one propylene from ion *m/z* 143. And ion *m/z* 58 is supposed to be from consecutive fragmentation of the parent ion. Although *m/z* 114 was also observed on the MS² spectrum of [Pr₂N=CHCH₂CH₃]⁺ (Fig. S6c, Supporting information), it should be due to the loss of C₂H₄ from the parent ion. Other two characteristic species at *m/z* 86 and 72 were produced by losing an ethylene and a propylene from ions *m/z* 144, respectively.

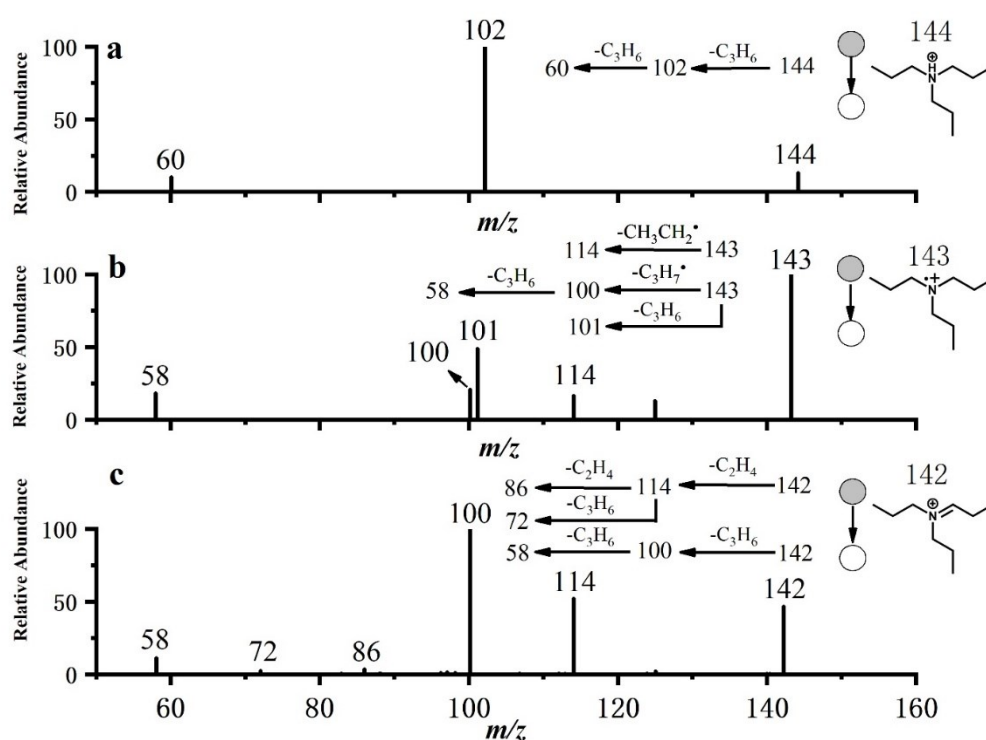


Fig. S6 Tandem mass spectra of a) protonated TPrA, b) TPrA^{•+} and c) [Pr₂N=CHCH₂CH₃]⁺. To obtain MS² spectra of *m/z* 144 and 142, the collision induced dissociation (CID) voltage was set as 30 V, and the maximum ion injection time was 30 ms. To obtain MS² spectrum of *m/z* 143, CID voltage was set as 35 V, and the maximum ion injection time was 30 ms.

Identification of the electrochemical formation of $\text{Ru}(\text{bpy})_3^+$

A mixture of $\text{Ru}(\text{bpy})_3^{2+}$ (50 μM) and TPrA (50 μM) in PBS (1 mM, pH = 7.5) solution was prepared. As shown in Fig. S7a (Supporting Information), the mass peaks of m/z 102, 144 and 285 are derived from the reagents, including NHPr_2 , TPrA and $\text{Ru}(\text{bpy})_3^{2+}$. When 0.8 V is applied to the working electrode, a new peak at m/z 570 can be observed on the spectrum (see Fig. S7b). It corresponds to the intermediate ion $\text{Ru}(\text{bpy})_3^+$, which is formed by $\text{Ru}(\text{bpy})_3^{2+}$ reduction with TPrA* (Scheme 1). Meanwhile, one can also find the TPrA oxidation products $[\text{Pr}_2\text{N}=\text{CHCH}_2\text{CH}_3]^+$ (m/z 142), TPrA^{*+} (m/z 143) and $[\text{NHPr}_2+\text{H}]^+$ (m/z 102, its relative abundance has significantly increased compared to that of the sample solution).

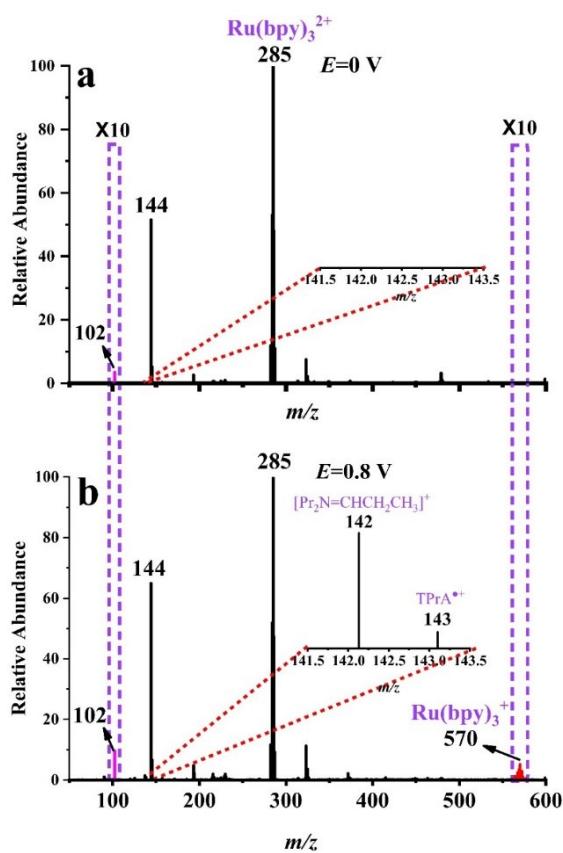


Fig. S7 EC/EASI mass spectra of $\text{Ru}(\text{bpy})_3^{2+}/\text{TPrA}$ system obtained at a) $E = 0$ V and b) $E = 0.8$ V.

Identification of the electrochemical formation of TPrA•

For the isolation with the ion deflector and subsequent neutral reionization (via the post-deflector ESI) MS detection of TPrA•, a sample solution of 100 ppm TPrA in nitrogen-saturated PBS buffer (1mM, pH=7.5) was prepared. For the radical trapping prior to the isolation and detection experiments, a mixed sample solution of 100 ppm TPrA and 0.1 mM DMPO in nitrogen-saturated PBS buffer (1mM, pH=7.5) was prepared.

The sample solution was injected into the EC cell at a fixed flow rate of 25 $\mu\text{L}/\text{min}$. The applied electrooxidation potential was 0.8 V vs. Ag/AgCl reference electrode and the gas pressure of EASI was ca. 60 psi. The temperature of the heating tube was set as 100 $^{\circ}\text{C}$, the voltage applied on the ion deflector was -5 kV and the voltage of ESI was 5 kV.

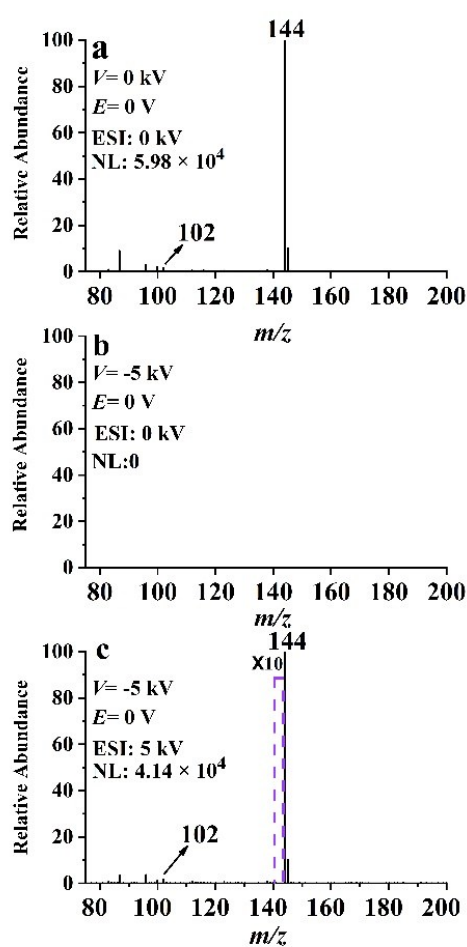


Fig. S8 EC-NR-MS spectra of TPrA sample solution (100 ppm), a) without deflection and ESI, b) with deflection but without ESI, and c) with deflection and ESI.

As shown in Fig. S9, in the cases of polarity switching of the deflector voltage, the relative abundances of the observed peaks remain unchanged.

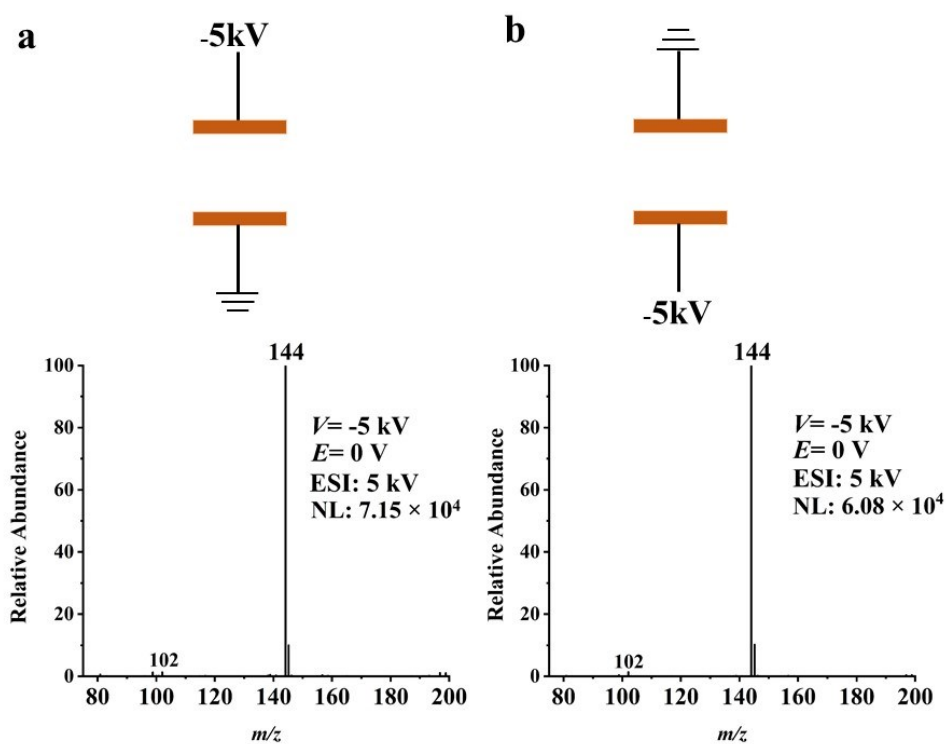
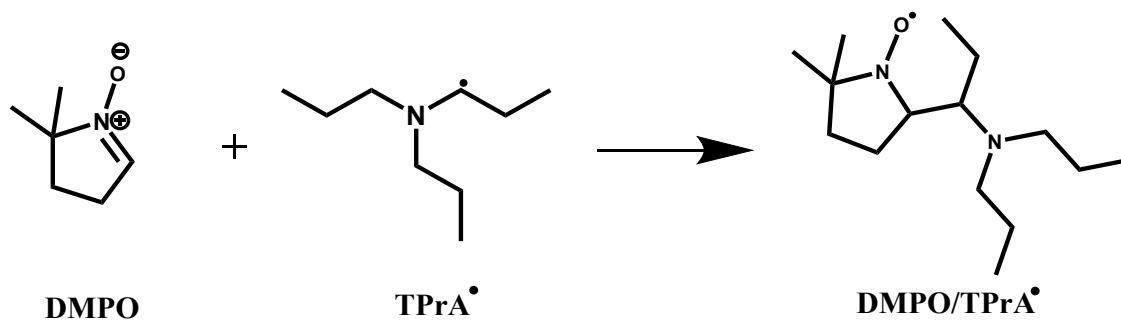


Fig. S9 Mass spectrum comparison of TPrA sample solution with polarity switching of the ion deflector.



Scheme S2 Mechanism of capturing TPrA[•] with DMPO.

As can be seen in Fig. S10b, The protonated spin adduct $[\text{DMPO}/\text{TPrA}^{\bullet}+\text{H}]^+$ generated several characteristic fragments at m/z 238, 228, 199 and 143. The loss of a H_2O and an ethylene from the parent ion produces the product ion at m/z 238 and 228, respectively. The ion at m/z 199 is also produced from the loss of a neutral species ($\text{C}_2\text{H}_3\text{NO}$) via a rearrangement process of the parent ion. The most abundant product ion at m/z 143 is formed from the protonated spin adduct $[\text{DMPO}/\text{TPrA}^{\bullet}+\text{H}]^+$ by losing a DMPO molecule.

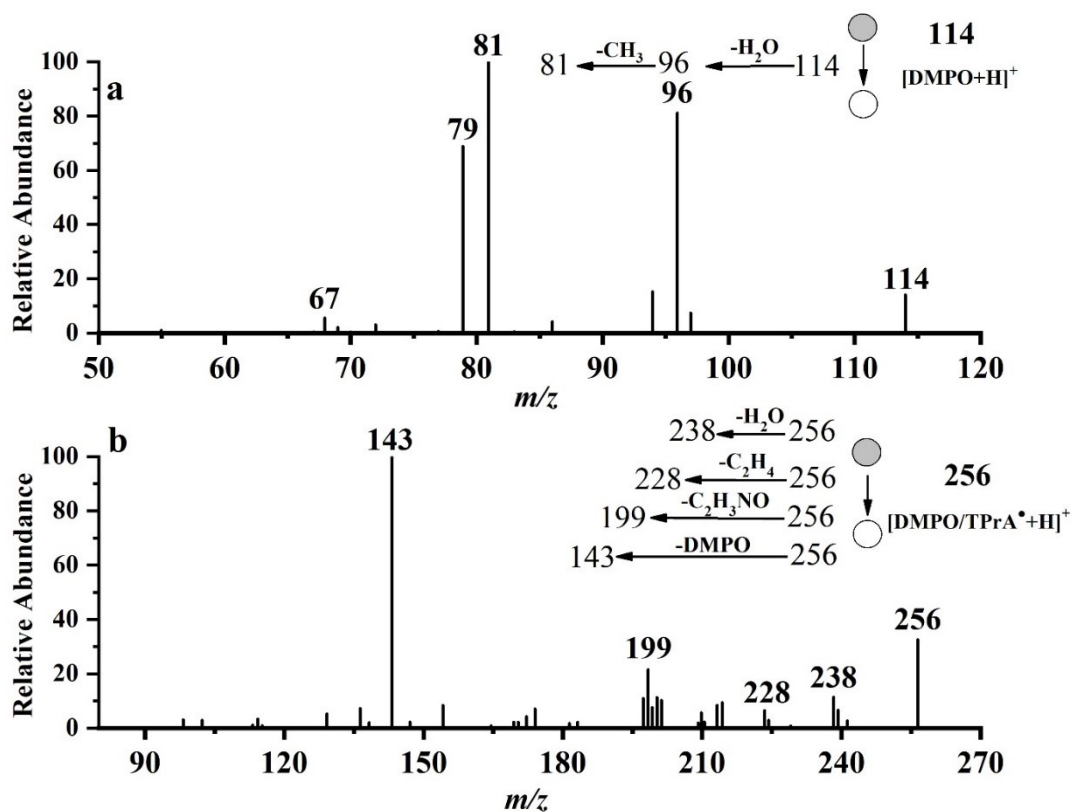


Fig. S10 Tandem mass spectra of protonated a) DMPO and b) DMPO/TPrA^{*}. To obtain MS² spectra of m/z 114, the collision induced dissociation (CID) voltage was set as 30 V, and the maximum ion injection time was 30 ms. To obtain MS² spectrum of m/z 256, CID voltage was set as 35 V, and the maximum ion injection time was 30 ms..

Specifically, the sample solution that has been studied in Fig. S7 was tested again with the addition of 0.1 mM DMPO, and the resulting MS spectra were shown in Fig. S11a (Supporting Information). The MS peaks of m/z 102, 114, 144 and 285 were corresponding to $[\text{NHPr}_2+\text{H}]^+$, $[\text{DMPO}+\text{H}]^+$, $[\text{TPrA}+\text{H}]^+$ and $\text{Ru}(\text{bpy})_3^{2+}$, respectively. When 0.8 V was applied to the working electrode, a new peak appeared in Fig. S11b, which was assigned to the protonated spin adduct $\text{DMPO}/\text{TPrA}^\bullet$ (m/z 256). However, in contrast with that shown in Fig. S7b, the peak of $\text{Ru}(\text{bpy})_3^+$ (produced from $\text{Ru}(\text{bpy})_3^{2+}$ by reduction with TPrA^\bullet) is absent at m/z 570 in Fig. S11b, suggesting that the reduction of $\text{Ru}(\text{bpy})_3^{2+}$ does not occur without TPrA^\bullet . Moreover, the relative abundance of m/z 102 in Fig. 11b is almost equal to that in Fig. S11a, and the peak of $[\text{Pr}_2\text{N}=\text{CHCH}_2\text{CH}_3]^+$ is not observed at m/z 142.

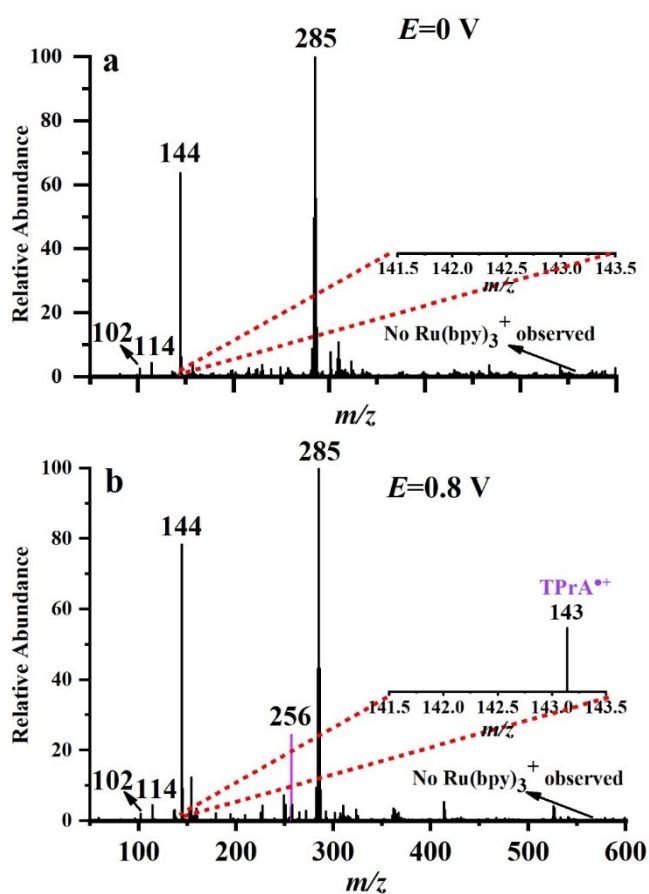


Fig. S11 EC/EASI mass spectra of $\text{Ru}(\text{bpy})_3^{2+}/\text{TPrA}$ system with DMPO obtained at a) $E = 0$ V and b) $E = 0.8$ V.

Identification of the electrochemical formation of DBAE^{•+}

As shown in Fig. S12a, the MS signal of 100 ppm DBAE in 1 mM PBS aqueous solution (pH=7.5) was determined, the peak at m/z 174 is assigned to the protonated DBAE. By holding the working electrode potential at 1.0 V, a new peak at m/z 118 appeared in Fig. S12b. The appearance of m/z 118 indicates the generation of 2-butylaminoethanol (2-BAE), which is the oxidation product of DBAE. In Fig. S12b, two new peaks appeared at m/z 172 and 173, corresponding to the DBAE iminium ion (DBAE-I) and radical cation DBAE^{•+}, respectively. Meanwhile, the structures of [DBAE+H]⁺, DBAE^{•+} and DBAE-I were characterized by tandem mass spectrometry (MS²) in Fig. S13. It should be pointed out that DBAE^{•+} is determined for the first time with EC-MS.

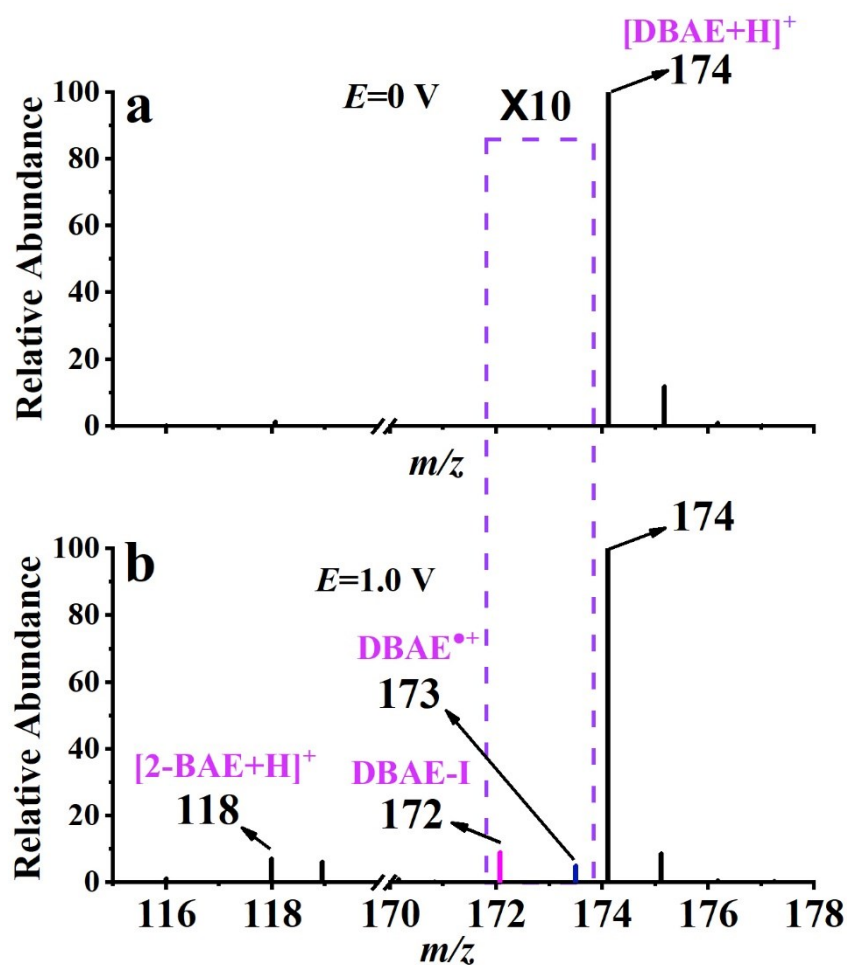


Fig. S12 MS spectra of 100 ppm DBAE in aqueous 1 mM PBS buffer, pH=7.5, scan rate=10 mV/s obtained at electrooxidation potential (E) of (a) 0 V and (b) 1.0 V.

As can be seen in Fig. S13a, $[\text{DBAE}+\text{H}]^+$ shows facile fragmentation by loss of butylene (at m/z 118). The peak at m/z 156 is owing to the $[\text{DBAE}+\text{H}]^+$ losing an H_2O . A small peak at m/z 100 is owing to an additional loss of butylene from m/z 156. In Fig. S13B the MS^2 of DBAE^{*+} generated typical fragments of m/z 130, 131, 116 and 88. The ions at m/z 131 and 130 are due to the loss of one propylene and one $\text{C}_3\text{H}_7^\bullet$ from DBAE^{*+} , respectively. Ion m/z 116 is assigned to the loss of one $\text{C}_4\text{H}_9^\bullet$ from DBAE^{*+} . Ion m/z 88 is supposed to be from consecutive fragmentation of the parent ion. MS^2 of DBAE-I generated typical fragments of m/z 130, 116, 100 and 88. The peak at m/z 130 is owing to the loss of propylene from DBAE-I and peak at m/z 88 is owing to an additional loss of propylene from m/z 130. Although m/z 116 was also observed on the MS^2 spectrum of DBAE-I , it should be due to the loss of butylene from DBAE-I . The peak at m/z 100 is owing to loss of $\text{C}_4\text{H}_8\text{O}$ from DBAE-I .

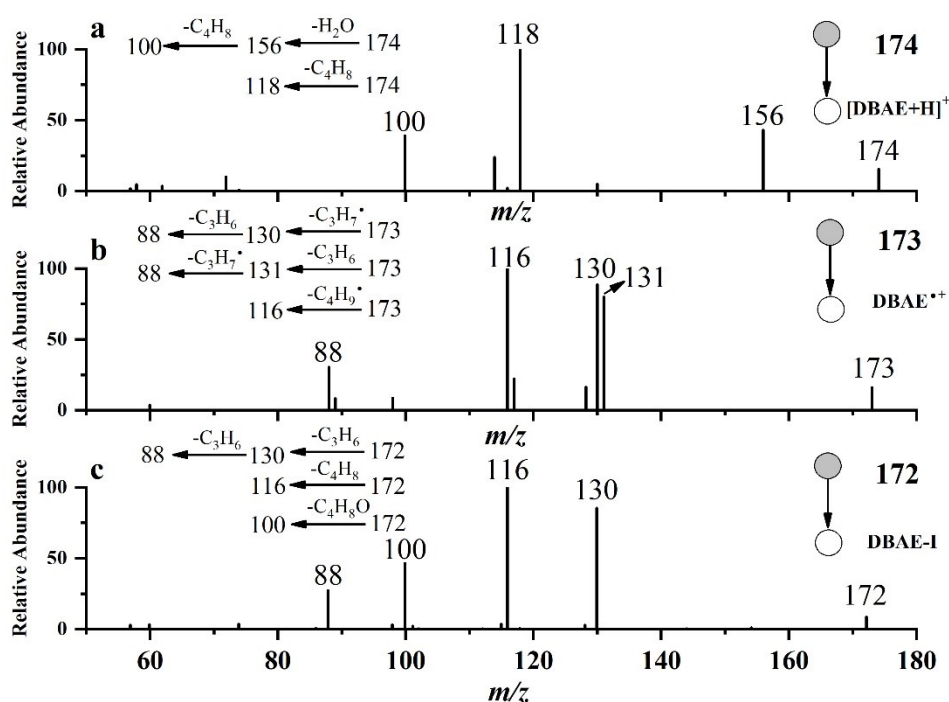
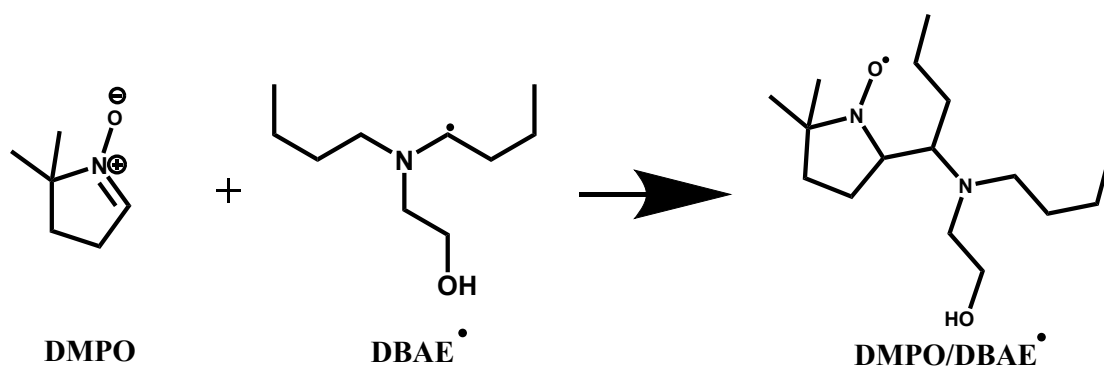


Fig. S13 Tandem mass spectra of a) protonated DBAE, b) DBAE^{*+} and c) DBAE-I . To obtain MS^2 spectra of m/z 174 and 172, the collision induced dissociation (CID) voltage was set as 30 V, and the maximum ion injection time was 30 ms. To obtain MS^2 spectrum of m/z 173, CID voltage was set as 35 V, and the maximum ion injection time was 30 ms.

Identification of the electrochemical formation of DBAE[•]



Scheme S3 Mechanism of capturing DBAE[•] with DMPO.

DMPO was used to capture DBAE• (Scheme S3). A solution containing 100 ppm DBAE, 1 mM PBS and 0.1 mM DMPO was used in the experiments with the deflector voltage (V) set at -5 kV. Fig. S14a and S14c were obtained in the absence of ESI, and thus there was no MS signal, meaning that all the ionic species were removed by the deflector. The mass peaks observed at m/z 174 and 114 in Fig. S14b are corresponding to the protonated DBAE and DMPO, respectively. When a potential (E) of 1.0 V was applied to the working electrode of the EC flow cell, a new peak (m/z 286) which should be assigned to the protonated spin adduct $[\text{DMPO}/\text{DBAE}^{\bullet}+\text{H}]^+$ is shown in Fig. S14d. The protonated spin adduct $[\text{DMPO}/\text{DBAE}^{\bullet}+\text{H}]^+$ was further characterized by MS² (see Fig. S15, Supporting Information). Evidently, the formation of the protonated spin adduct $[\text{DMPO}/\text{DBAE}^{\bullet}+\text{H}]^+$ further verified the generation of DBAE•.

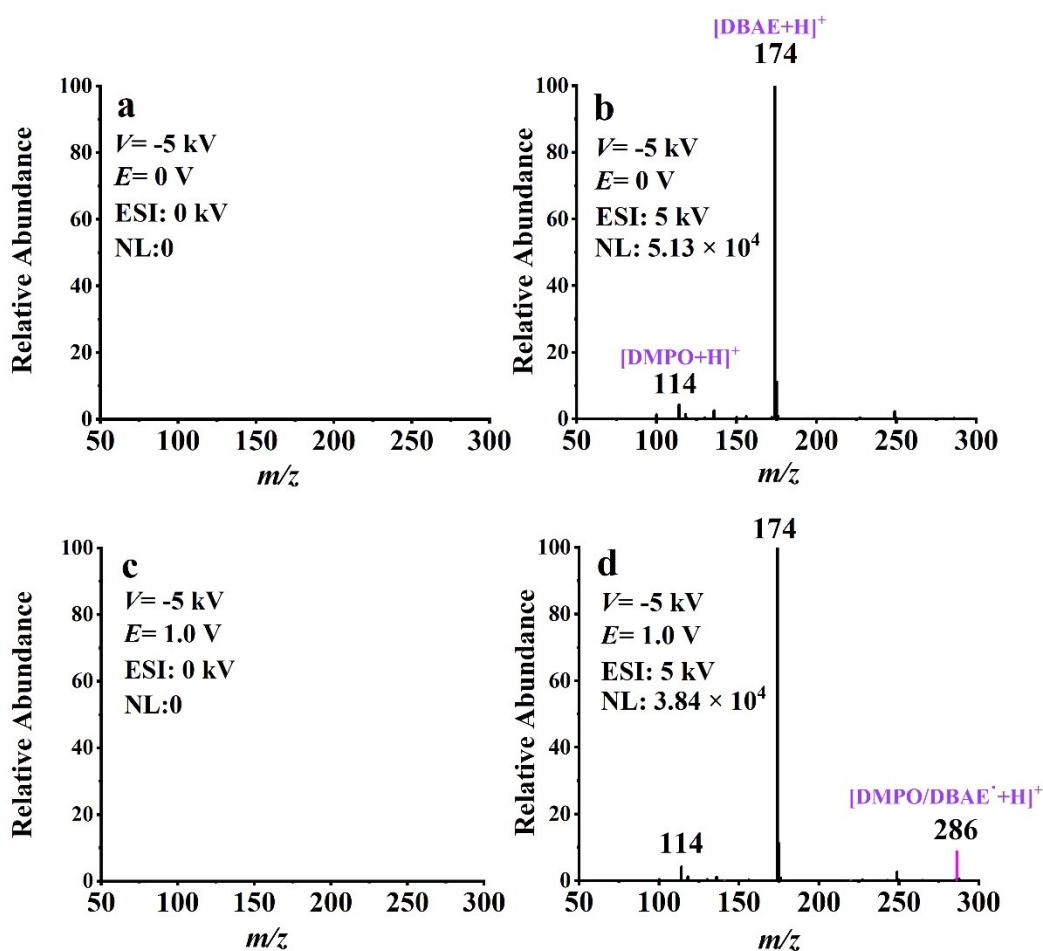


Fig. S14 EC-NR-MS spectra of 100 ppm DBAE solution containing 0.1 mM DMPO and 1mM PBS (pH=7.5), a) $E = 0$ V without ESI, b) $E = 0$ V with ESI, c) $E = 1.0$ V without ESI, and d) $E = 1.0$ V with ESI. E is the applied electrooxidation potential for DBAE and the ionization voltage of ESI is 5 kV.

As can be seen in Fig. S15, The protonated spin adduct $[\text{DMPO/DBAE}^{\bullet}+\text{H}]^+$ generated several characteristic fragments at m/z 269, 230, 188 and 156. The loss of OH and an butylene from the parent ion produces the product ion at m/z 269 and 230, respectively. The ion at m/z 188 is produced from the loss of a propylene from m/z 230. The product ion at m/z 156 is formed from the ion at m/z 269 by losing a DMPO moiety.

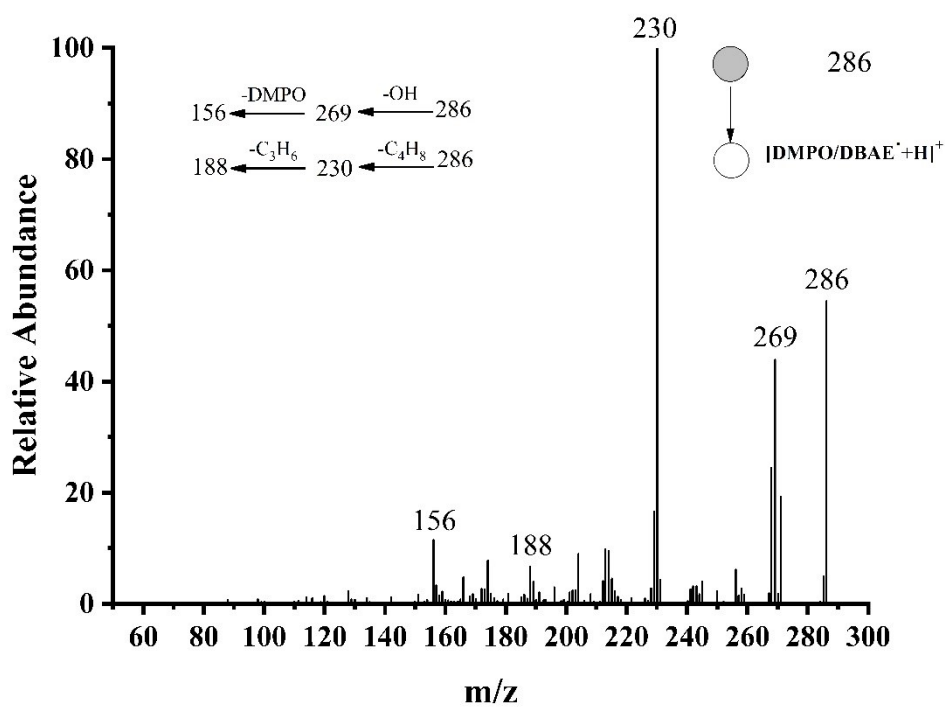
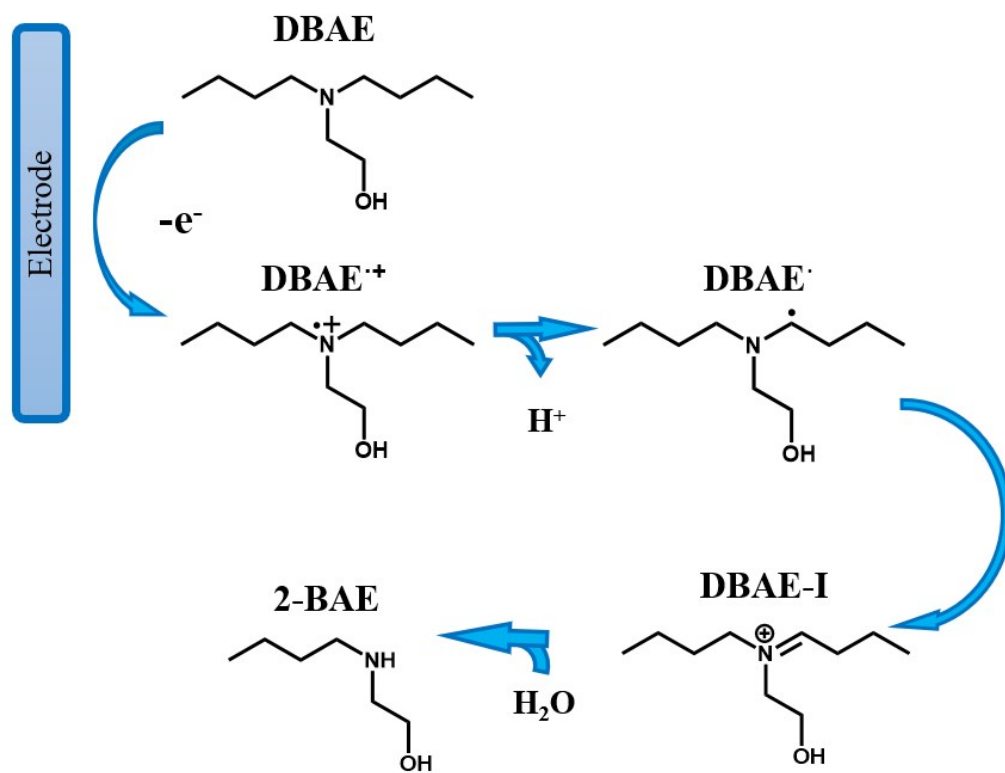


Fig. S15 Tandem mass spectra of protonated $\text{DMPO/DBAE}^{\bullet}$, CID voltage was set as 30 V, and the maximum ion injection time was 30 ms..



Scheme S4 Electrooxidation pathway of DBAE at potential of 1.0 V.

Identification of the electrochemical formation of TEA^{•+}

We tried to capture TEA^{•+}. As shown in Fig. S16a, the MS signal of 100 ppm TEA in 1 mM PBS aqueous solution (pH=7.5) was determined, the major peak at m/z 150 is assigned to the protonated TEA. By holding the working electrode potential at 1.0 V, a new peak at m/z 106 appeared in Fig. S16b. The appearance of m/z 106 indicating the generation of diethanolamine (DEA), which is the oxidation product of TEA. In Fig. S16b, two new peaks appeared at m/z 148 and 149, corresponding to the TEA iminium ion (TEA-I) and radical cation TEA^{•+}, respectively. Meanwhile, the structural characterization of [TEA+H]⁺, TEA^{•+} and TEA-I was achieved by tandem mass spectrometry (MS²) as shown in Fig. S17. It should be pointed out that TEA^{•+} is determined for the first time with EC-MS.

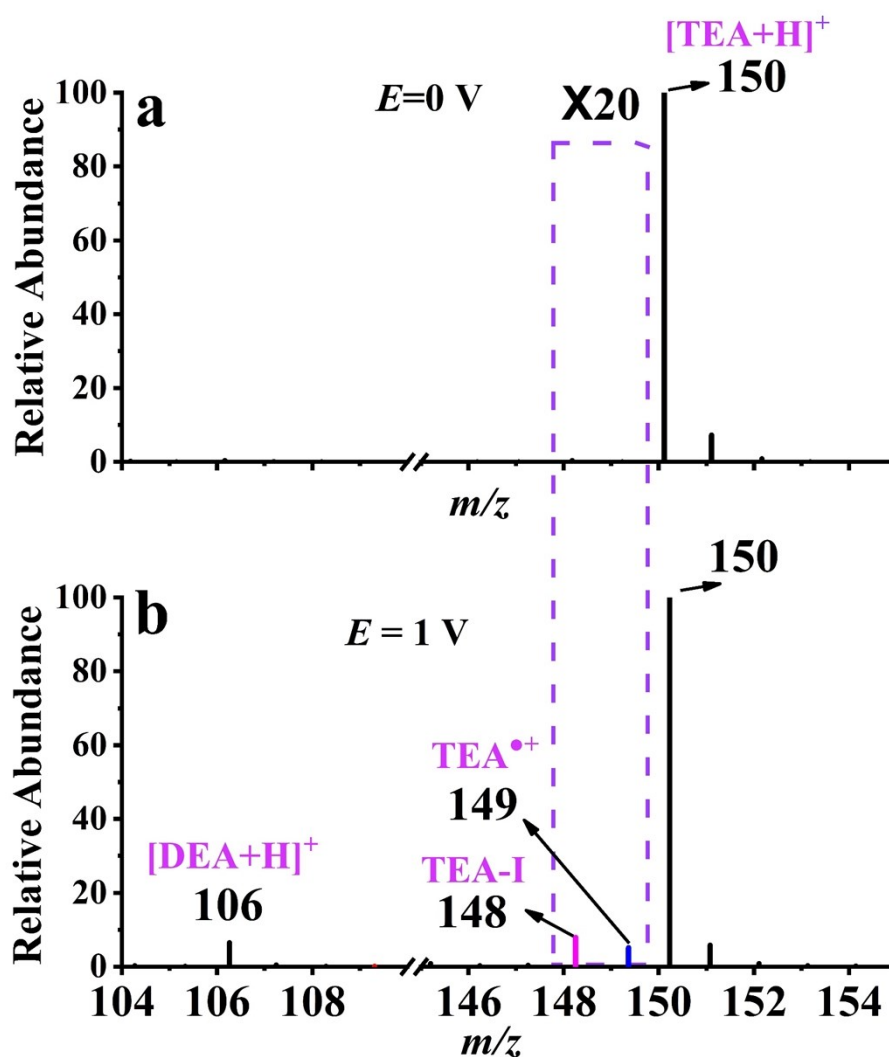


Fig. S16 MS spectra of 100 ppm TEA in aqueous 1 mM PBS buffer, pH=7.5, scan rate=10 mV/s obtained at electrooxidation potential (E) of (a) 0 V and (b) 1.0 V.

As shown in Fig. S17a, $[\text{TEA}+\text{H}]^+$ shows facile fragmentation by loss of H_2O (at m/z 132). A small peak at m/z 88 is owing to an additional loss of $\text{C}_2\text{H}_4\text{O}$ from m/z 132. As shown in Fig. S17b the MS^2 of TEA^{*+} generated typical fragments of m/z 131, 132, and 88. The ions at m/z 131 and 132 are due to the loss of H_2O and OH from TEA^{*+} , respectively. Ion m/z 88 is assigned to the loss of one $\text{C}_4\text{H}_8\text{O}$ from m/z 132. MS^2 of TEA-I generated typical fragments of m/z 130 and 88. The peak at m/z 130 is owing to the loss of H_2O from TEA-I and peak at m/z 88 is owing to loss of two CH_2O from TEA-I .

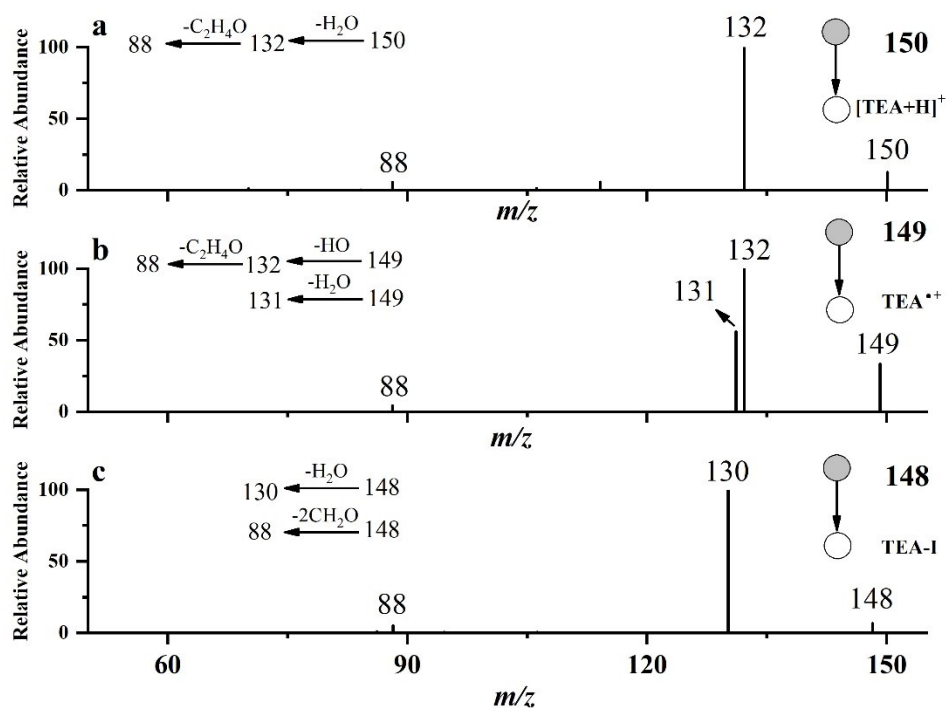
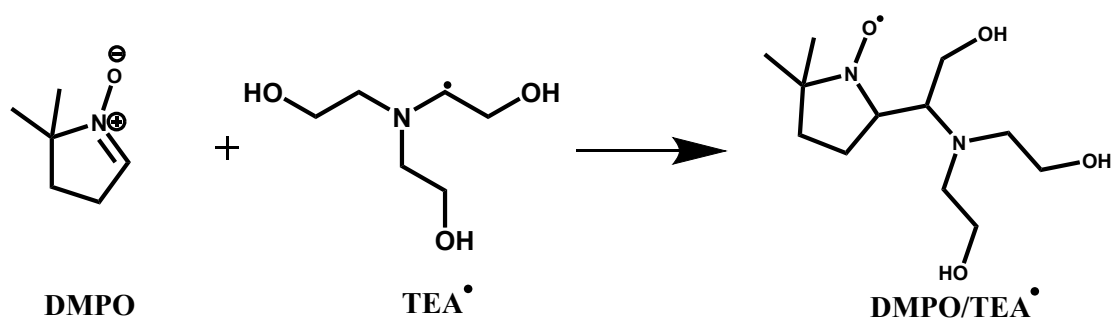


Fig. S17 Tandem mass spectra of a) protonated TEA, b) TEA^{*+} and c) TEA-I . To obtain MS^2 spectra of m/z 150 and 148, the collision induced dissociation (CID) voltage was set as 30 V, and the maximum ion injection time was 30 ms. To obtain MS^2 spectrum of m/z 149, CID voltage was set as 35 V, and the maximum ion injection time was 30 ms.

Identification of the electrochemical formation of TEA[•]



Scheme S5 Mechanism of capturing TEA[•] with DMPO.

A solution containing 100 ppm TEA, 1 mM PBS and 0.1 mM DMPO was used in the experiments with a deflector voltage (V) of -5 kV. Fig. S18a and S18c shows that in the absence of ESI, no MS signal was observed. It means that all the ionic species were removed by the deflector. In Fig. S18b, the peaks observed at m/z 150 and 114 are corresponding to the protonated TEA and DMPO, respectively. When a potential (E) of 1.0 V was applied to the working electrode of the EC flow cell, a new peak at m/z 262, assigned to the protonated spin adduct $[\text{DMPO/TEA}^{\bullet+}\text{H}]^+$, appears in Fig. S18d.

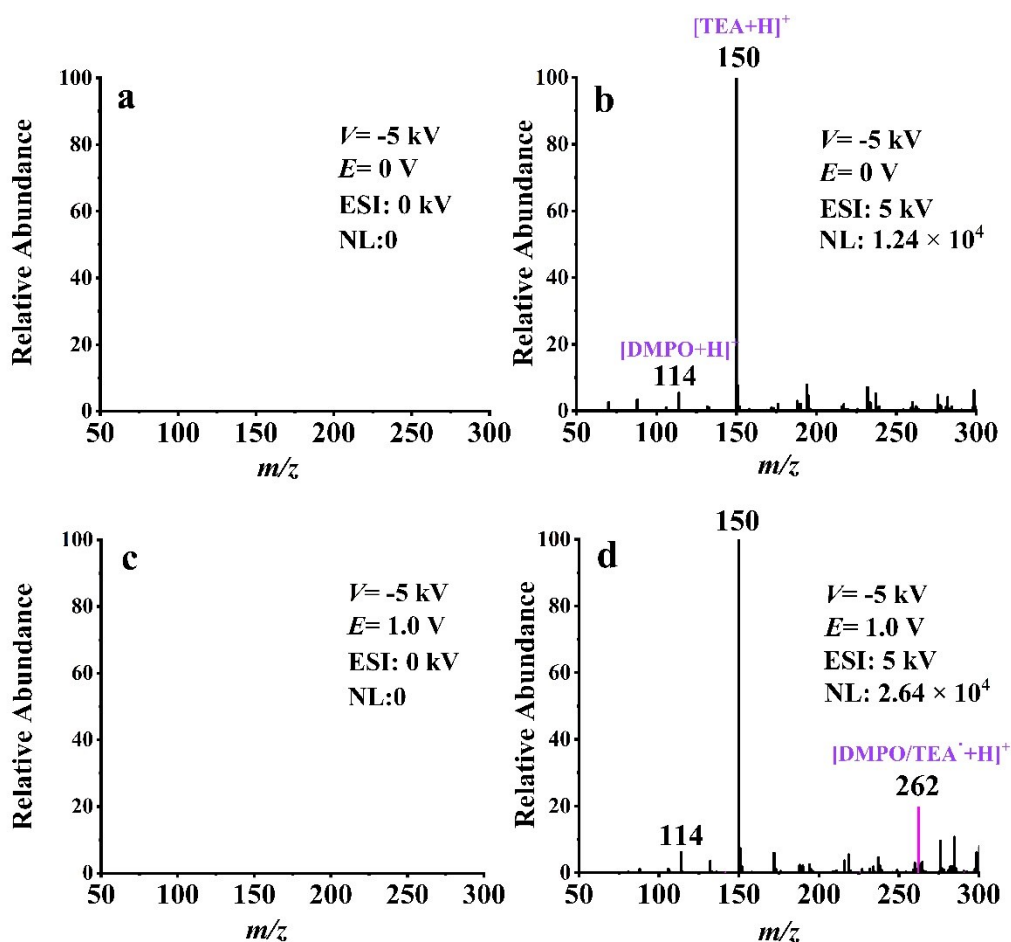


Fig. S18 EC-NR-MS spectra of 100 ppm TEA solution containing 0.1 mM DMPO and 1mM PBS (pH=7.5), a) $E = 0$ V without ESI, b) $E = 0$ V with ESI, c) $E = 1.0$ V without ESI, and d) $E = 1.0$ V with ESI. E is the applied electrooxidation potential for TEA and the ionization voltage of ESI is 5 kV.

As can be seen in Fig. S19, The protonated spin adduct $[\text{DMPO/DBAE}^{\bullet}+\text{H}]^+$ generated several characteristic fragments at m/z 244, 218, 188, 157 and 113. The ion at m/z 244 is produced from the loss of a H_2O from m/z 262. The ion at m/z 218 is produced from the loss of a $\text{C}_2\text{H}_4\text{O}$ from m/z 262. The product ion at m/z 188 is formed from the ion at m/z 218 by losing a CH_2O and the ion at m/z 157 is due to the loss of $\text{CH}_3\text{O}^{\bullet}$ from the ion at m/z 188. The ion at 113 is formed due to the loss of $\text{C}_6\text{H}_{15}\text{NO}_3$ from the ion at m/z 262.

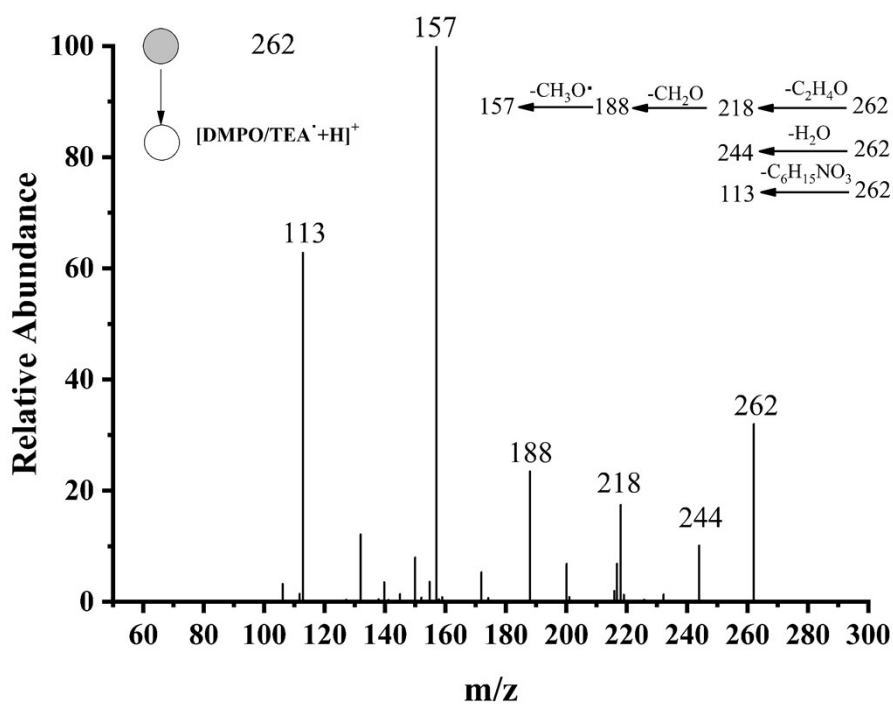
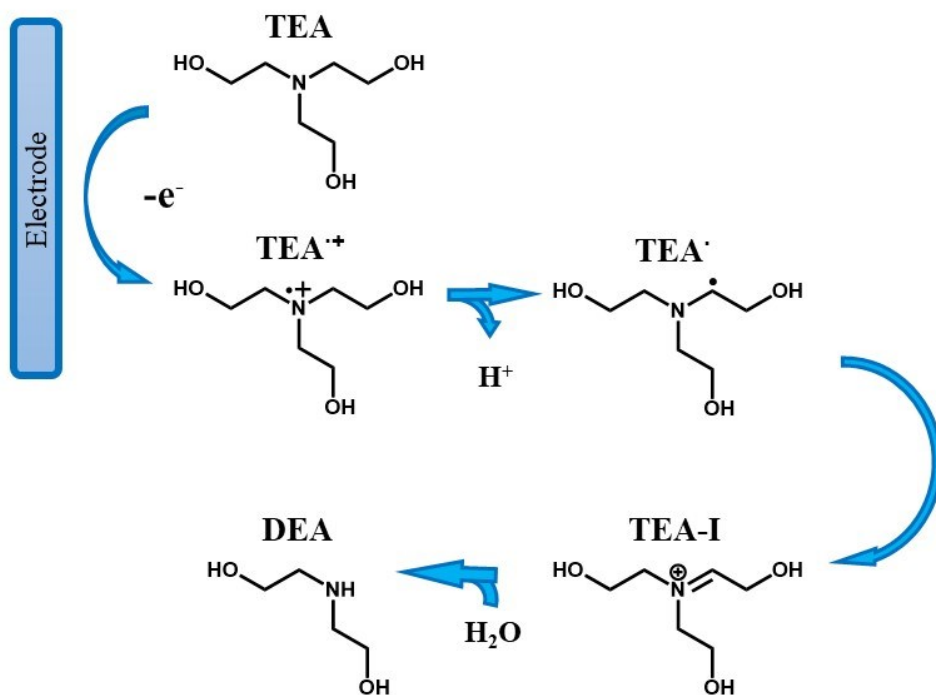


Fig. S19 Tandem mass spectra of protonated $\text{DMPO/TEA}^{\bullet}$, CID voltage was set as 30 V, and the maximum ion injection time was 30 ms..



Scheme S6 Electrooxidation pathway of TEA at potential of 1.0 V

Reference

1. W. Miao, J. P. Choi and A. J. Bard, *J. Am. Chem. Soc.*, 2002, **124**, 14478-14485.
2. R. Qiu, X. Zhang, H. Luo and Y. Shao, *Chem. Sci.*, 2016, **7**, 6684-6688.
3. J. Hu, N. Zhang, P. K. Zhang, Y. Chen, X. Xia, H. Chen and J. Xu, *Angew. Chem. Int. Ed.*, 2020, **59**, 18244-18248.